Research article

Small-molecule modulators of Hedgehog signaling: identification and characterization of Smoothened agonists and antagonists

Maria Frank-Kamenetsky*, Xiaoyan M Zhang*, Steve Bottega*, Oivin Guicherit*, Hynek Wichterle†, Henryk Dudek*, David Bumcrot*, Frank Y Wang*, Simon Jones*, Janine Shulok*, Lee L Rubin* and Jeffery A Porter*

Addresses: *Curis, Inc., 61 Moulton Street, Cambridge, MA 02138, USA. †Columbia University, College of Physicians and Surgeons, 701 West 168 Street, New York, NY 10032, USA.

Correspondence: Jeffery A Porter. E-mail: jporter@curis.com

Abstract

Background: The Hedgehog (Hh) signaling pathway is vital to animal development as it mediates the differentiation of multiple cell types during embryogenesis. In adults, Hh signaling can be activated to facilitate tissue maintenance and repair. Moreover, stimulation of the Hh pathway has shown therapeutic efficacy in models of Parkinson's disease and diabetic neuropathy. The underlying mechanisms of Hh signal transduction remain obscure, however: little is known about the communication between the pathway suppressor Patched (Ptc), a multipass transmembrane protein that directly binds Hh, and the pathway activator Smoothened (Smo), a protein that is related to G-protein-coupled receptors and is capable of constitutive activation in the absence of Ptc.

Results: We have identified and characterized a synthetic non-peptidyl small molecule, Hh-Ag, that acts as an agonist of the Hh pathway. This Hh agonist promotes cell-type-specific proliferation and concentration-dependent differentiation *in vitro,* while *in utero* it rescues aspects of the Hh-signaling defect in *Sonic hedgehog*-null, but not *Smo*-null, mouse embryos. Biochemical studies with Hh-Ag, the Hh-signaling antagonist cyclopamine, and a novel Hh-signaling inhibitor Cur61414, reveal that the action of all these compounds is independent of Hh-protein ligand and of the Hh receptor Ptc, as each binds directly to Smo.

Conclusions: Smo can have its activity modulated directly by synthetic small molecules. These studies raise the possibility that Hh signaling may be regulated by endogenous small molecules *in vivo* and provide potent compounds with which to test the therapeutic value of activating the Hh-signaling pathway in the treatment of traumatic and chronic degenerative conditions.

Background

The *hedgehog* (*hh*) gene was identified two decades ago in *Drosophila* as a critical regulator of cell-fate determination during embryogenesis [1]. Subsequent work in several model systems has defined and characterized the *Hh* gene family that encodes highly conserved secreted signaling proteins (for review see [2]). Hedgehog (Hh) proteins are synthesized as approximately 45 kDa precursors that autoprocess in an unprecedented fashion, resulting in the covalent attachment of a cholesterol moiety to the amino-terminal half of the precursor [2]. This processed amino-terminal domain, Hh-Np, is responsible for the activation of a unique and complex signaling cascade that is essential for controlling cell fate throughout development and into adulthood [2]. In mammals there are three Hh-family proteins: Sonic (Shh), Indian (Ihh), and Desert (Dhh). Gene-targeting experiments in mice have demonstrated that the development and patterning of essentially every major organ requires input from the Hh pathway [2].

In vitro culture systems of neuronal tissues have been used to characterize the biology of the Hh-signaling pathway. Most notably, the neural-plate explant assay has defined the concentration-dependent role that ventrally expressed Shh plays in opposing dorsally expressed bone morphogenetic proteins (BMPs) to pattern the neural tube [2]. The assay demonstrates that the Hh-signaling cascade can distinguish between small concentration differences in the Hh ligand to instruct the differentiation of specific neuronal cell types. Additional insights have been gained by utilizing cultures of postnatal cerebellar neuron precursors [2]. These studies have shown that Hh patterns the cerebellum by promoting proliferation of the granule neuron precursors. Given the role that Hh signaling plays in promoting progenitor-cell proliferation, it is not surprising that misregulation of Hh signaling has been implicated in the biology of certain cancers, in particular basal cell carcinoma (BCC) and medulloblastoma.

The Hh-signaling pathway comprises three main components: the Hh ligand; a transmembrane receptor circuit composed of the negative regulator Patched (Ptc) plus an activator, Smoothened (Smo); and finally a cytoplasmic complex that regulates the Cubitus interruptus (Ci) or Gli family of transcriptional effectors. Additional pathway components are thought to modulate the activity or subcellular distribution of these molecules [2]. There is positive and negative feedback at the transcriptional level as the *Gli1* and *Ptc1* genes are direct transcriptional targets of activation of the pathway.

Smo is a seven-pass transmembrane protein with homology to G-protein-coupled receptors (GPCRs), while Ptc is a twelve-pass transmembrane protein that resembles a channel or transporter. Consistent with its role as an essential pathway inhibitor, removal of Ptc renders the Hh pathway constitutively 'on', independent of the Hh ligand. Similarly, specific point mutations in the transmembrane helices of Smo are capable of constitutively stimulating the pathway, effectively bypassing Ptc inhibition [3]. At present, a controversy surrounds the mechanism by which Ptc inhibits Smo. Although early studies suggested a simple, direct, stoichiometric regulation, more recent data support a more complicated indirect or catalytic model [2]. And although it has been demonstrated that Hh directly interacts with [4] and destabilizes [5] Ptc, the downstream molecular events remain obscure. In particular, little is known about the means by which Ptc exerts its inhibitory effect on Smo, or how Smo communicates with the cytoplasmic Ci/Gli transcription factor complex.

Through a 'chemical genetic' approach of identifying and studying the mechanism of action of small-molecule agonists (and antagonists), we hoped to uncover some of the complexities of the Hh-signaling system. Small-molecule modulators of growth-factor pathways have proven valuable in providing enhanced understanding of the intracellular events that occur subsequent to receptor activation, and in establishing the biological functions of these pathways [6-8]. In Hh signaling, multiple insights have been gained through the use of the plant-derived Hh antagonist cyclopamine [9-16] and a recently identified synthetic small-molecule Hh-signaling inhibitor, Cur61414 [17]. Interestingly, these specific inhibitors of Hh signaling appear to function downstream of Ptc but their precise molecular target(s) and mechanism of action are unknown.

Although genetic manipulations involving gain-of-function point mutations of Smo [3] have demonstrated that the pathway can be activated independently of Hh ligand, no small molecules with this capability have been identified. Indeed, it has proven difficult to identify small-molecule agonists of any signaling pathway activated by a protein ligand. Two examples have recently been described, however. One involved identification of a non-peptide activator of the granulocyte colony-stimulating factor (GCSF) pathway that appeared to act via receptor oligomerization [18]. Another report described a small-molecule activator of the insulin-signaling pathway that also acts at the level of the receptor [19].

Since the Hh receptor, Ptc, serves to inhibit signaling, a small-molecule pathway activator would need to be capable of one of the following: first, interfering with the inhibitory effect that Ptc exerts on Smo; second, activating Smo without affecting Ptc; or third, activating the pathway downstream of

Smo. Identifying small molecules with any of these activities would provide useful information concerning the details of Hh signaling and would also provide a simple means of modulating activity of the pathway *in vivo* or *in vitro*.

In this article, we show that a non-peptidyl small-molecule agonist of Hh signaling has been identified that has all the known signaling properties of the recombinant Hh protein. But this agonist, unlike Hh protein, appears to bypass the Ptc-regulatory step, by interacting directly with Smo. Furthermore, studies with the agonist and several antagonists of Hh signaling suggest that Smo can be activated or inhibited by direct interaction with small-molecule ligands. These observations suggest that the Ptc-Smo receptor circuit may incorporate native small-molecule ligands in the regulation of Hh signaling.

Results
Isolation of Hh agonists by high-throughput screening
To identify small-molecule agonists of Hh signaling, we established a mammalian-cell-based assay. After testing several cell lines for Hh-dependent induction of the target genes *Ptc1* and *Gli1* [2], we identified C3H10T1/2 and TM3 cells as optimal responders. We then introduced into each line a plasmid containing a luciferase reporter downstream of multimerized Gli binding sites and a minimal promoter [20]. An isolated stable clone of the 10T1/2 cell transfectants (referred to as clone S12) gave a 10-20-fold up-regulation of luciferase activity (Figure 1a) when stimulated with Hh protein [21] for 24 hours. Using this assay system, we screened 140,000 synthetic compounds at a concentrations of 2-5 μM and isolated several putative agonists. One of these molecules - Hh-Ag 1.1 (Figure 1a,b) - was studied further. Hh-Ag 1.1 exhibited half-maximal stimulation (EC$_{50}$) at around 3 μM, and an activation maximum (A$_{max}$) of approximately 35% compared to the Hh protein control (Figure 1a). In the presence of sub-threshold signaling levels of Hh protein (0.3 nM), the EC$_{50}$ of Hh-Ag 1.1 was reduced to around 0.4 μM and the A$_{max}$ approached 70% (Figure 1a).

We next tested whether expression of endogenous Hh-responsive genes was stimulated by the agonist. Using quantitative PCR, Hh-Ag 1.1 was shown clearly to elevate the expression of *Gli1* and *Ptc1* in a dose-dependent manner (Figure 1c).

Chemical modifications increase potency
In an effort to improve the potency of Hh-Ag 1.1, over 300 derivatives were synthesized and tested in the cell-based reporter assay. The relative potencies of the most active

derivatives - 1.2, 1.3, 1.4 and 1.5 - are shown in Figure 1d. The most potent, Hh-Ag 1.5, had an EC$_{50}$ of approximately 1 nM. Thus, potency was increased over 1000-fold by chemical modification. The structures of compounds 1.2 and 1.3 are shown in Figure 1e. Hh-Ag 1.2 was the most stable derivative *in vivo* and *in vitro* (data not shown) and was used for most cell-based assays. Hh-Ag 1.3 showed lower toxicity in embryonic tissue cultures (data not shown) and was used for the neural plate explant assays described below. These experiments suggest that the agonist may have many of the properties of the Hh ligand. To specifically test this, we used two established *in vitro* assay systems that detect the effects of Hh on primary neuronal precursors.

In vitro assay of neuronal precursors
Proliferation activity of the agonist
It has recently been shown that primary neonatal cerebellar granule neuron (CGN) precursors proliferate in response to Hh stimulation [2]. To determine whether the Hh agonist could elicit this response, we monitored [^{3}H]-thymidine incorporation of cultured rat CGN precursors treated with Hh protein, Hh-Ag 1.1, Hh-Ag 1.2, or vehicle (DMSO). The original active molecule, Hh-Ag 1.1, stimulated thymidine incorporation at 5 μM, but not at 1.75 μM (Figure 1f). The extent of proliferation was around 50% of that seen with a high dose of Hh protein (50 nM). Hh-Ag 1.2 stimulated proliferation at 300 nM and 100 nM to levels comparable to those seen with Hh protein (Figure 1f). These data demonstrate that the agonists can elicit a biological response in primary cells similar to that produced by Hh protein.

Morphogenic activity of the agonist
Neural progenitors within the intermediate region of the chick neural plate (Figure 2a) respond to increasing concentrations of Hh protein by adopting specific fates. The identity of these cells can be assessed by their distinct expression patterns of a set of transcription factors [2]. Three of these transcription factors - Pax7, MNR2 and Nkx2.2 - whose expression is differentially sensitive to increasing concentrations of Hh protein were assayed in response to varying concentrations of the agonist (Hh-Ag 1.3). The dorsal spinal cord marker Pax7 is normally repressed by low concentrations of Hh [22]. Pax7 expression was extinguished by 1-10 nM agonist (Figure 2b-f). Higher concentrations of agonist (10-200 nM) induced expression of the motor neuron progenitor marker MNR2 (Figure 2b,g-j), and yet higher concentrations (20 nM–1 μM) induced the most ventral interneuron progenitor marker Nkx2.2 (Figure 2b,k-n). This dose-dependent profile of expression closely resembles the response achieved by increasing concentrations of Hh protein [22-24], demonstrating that the Hh agonist mimics the concentration-dependent inductive activity of Hh on neural precursors.
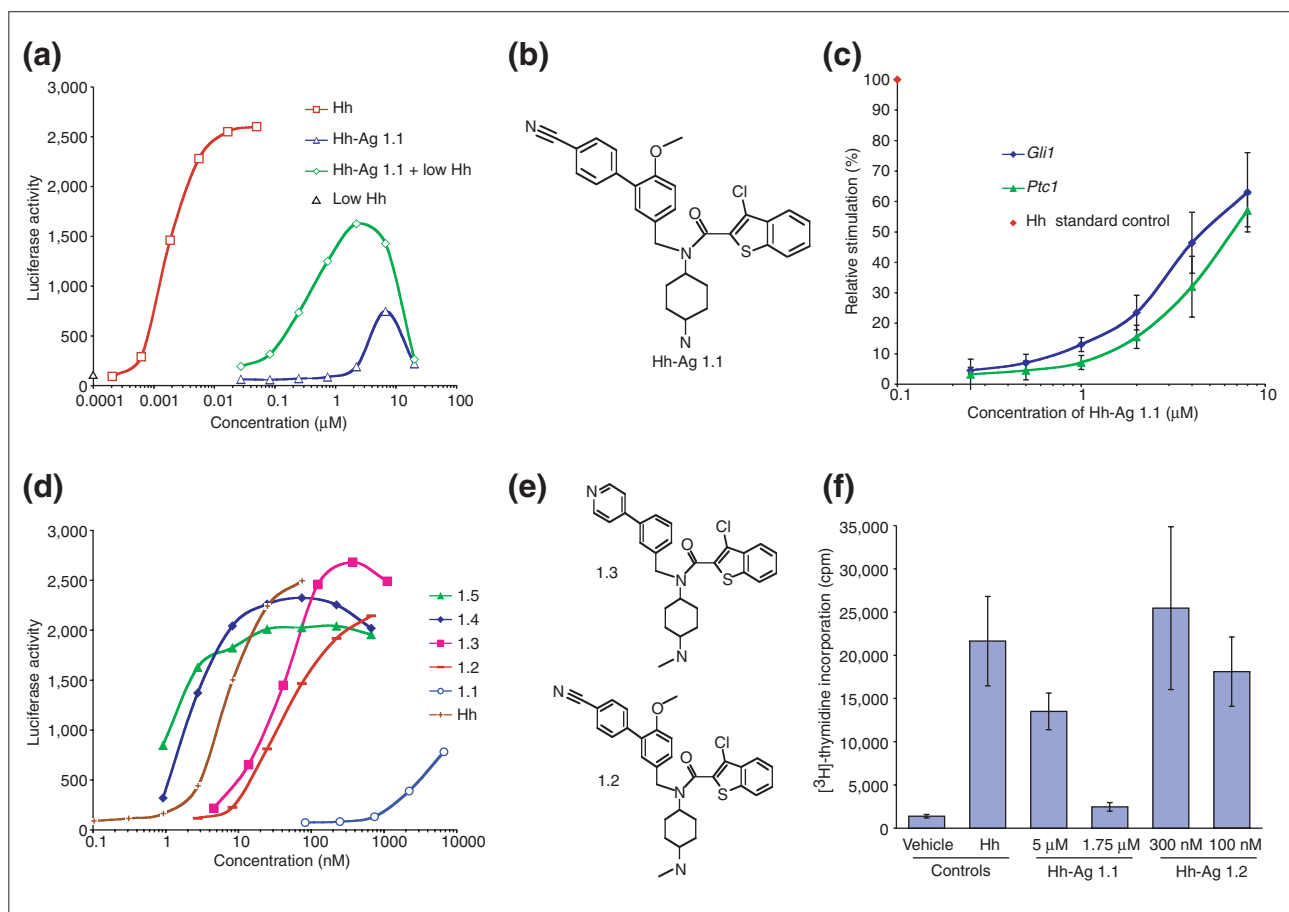
Figure 1

A Hh-signaling agonist identified in a cell-based small-molecule screen. **(a)** A luciferase-based reporter assay of Hh signaling, showing a dose-response curve for the following: Hh protein (Hh); the small-molecule agonist Hh-Ag 1.1; Hh-Ag 1.1 in the presence of 0.3 nM Hh protein (Hh-Ag 1.1 + low Hh); or 0.3 nM Hh protein alone (low Hh). Data points represent the averages (n = 4) with standard deviations less than 15%. **(b)** The structure of Hh-Ag 1.1. **(c)** The output of a quantitative PCR analysis of *Ptc1* and *Gli1* mRNA levels from C3H10T1/2 cells exposed for 18 hours to an increasing dose of Hh-Ag 1.1. Data are graphed as relative activation versus Hh-Ag 1.1 concentration (μM). The 0 to 100% range was set using data from cells treated with 0 or 25 nM Hh protein; fold inductions for levels of *Ptc1* and *Gli1* mRNA were determined using *GAPDH* mRNA levels as internal standards. Each data point represents an average (n = 4) with standard deviation shown by error bars. **(d)** A luciferase-based reporter assay of Hh signaling showing dose-response curves (with concentrations in nM) for Hh protein and the five agonist compounds Hh-Ag 1.1, 1.2, 1.3, 1.4 and 1.5. Graphs are representative of multiple assays of these compounds. Data points represent the averages (n = 2) with standard deviations less than 15%. **(e)** Structures of Hh-agonist derivatives; 1.2 is a methylated analog, and 1.3 a methylated analog with a para-pyridyl moiety. **(f)** A proliferation assay of Hh-responsive primary neuronal precursors from postnatal day 4 rat cerebellum. [³H]-thymidine incorporation was measured 24 hours after the addition of the vehicle dimethyl sulfoxide ('vehicle'), Hh protein, or agonist. Hh protein was tested at 50 nM; Hh-Ag 1.1 was added at 5 and 1.75 μM; Hh-Ag 1.2 was added at 300 and 100 nM. Data points represent the averages (n = 4) with standard deviations depicted with error bars.

Activity of the agonist *in vivo*

To explore the site of action of the Hh agonist within the Hh pathway, we developed an *in vivo* assay for the agonist that would allow us to test its activity in *Shh*- and *Smo*-mutant mouse embryos *in utero*. First, we compared the expression of *Ptc1* in vehicle- and agonist-treated *Ptc1^{lacZ/+}* mouse embryos [25]. The *Ptc1^{lacZ/+}* mouse expresses β-galactosidase under control of *Ptc1*-regulatory elements and thus reports Hh-pathway activity in mouse tissues. Hh-Ag 1.2 (Figure 1e) was

chosen for study on the basis of its relatively low toxicity, long serum half-life and ability to cross the placenta (data not shown). Hh-Ag 1.2 was delivered by oral gavage to pregnant mice at 7.5 and 8.5 days post coitum (7.5 and 8.5 dpc). Embryos were collected at embryonic day (E) 9.5 and analyzed by staining with the β-galactosidase chromogenic substrate X-gal. In vehicle-treated embryos, *Ptc1* expression was confined primarily to the ventral neural tube (Figure 3a,c). In embryos treated with Hh-Ag 1.2, however, expression of
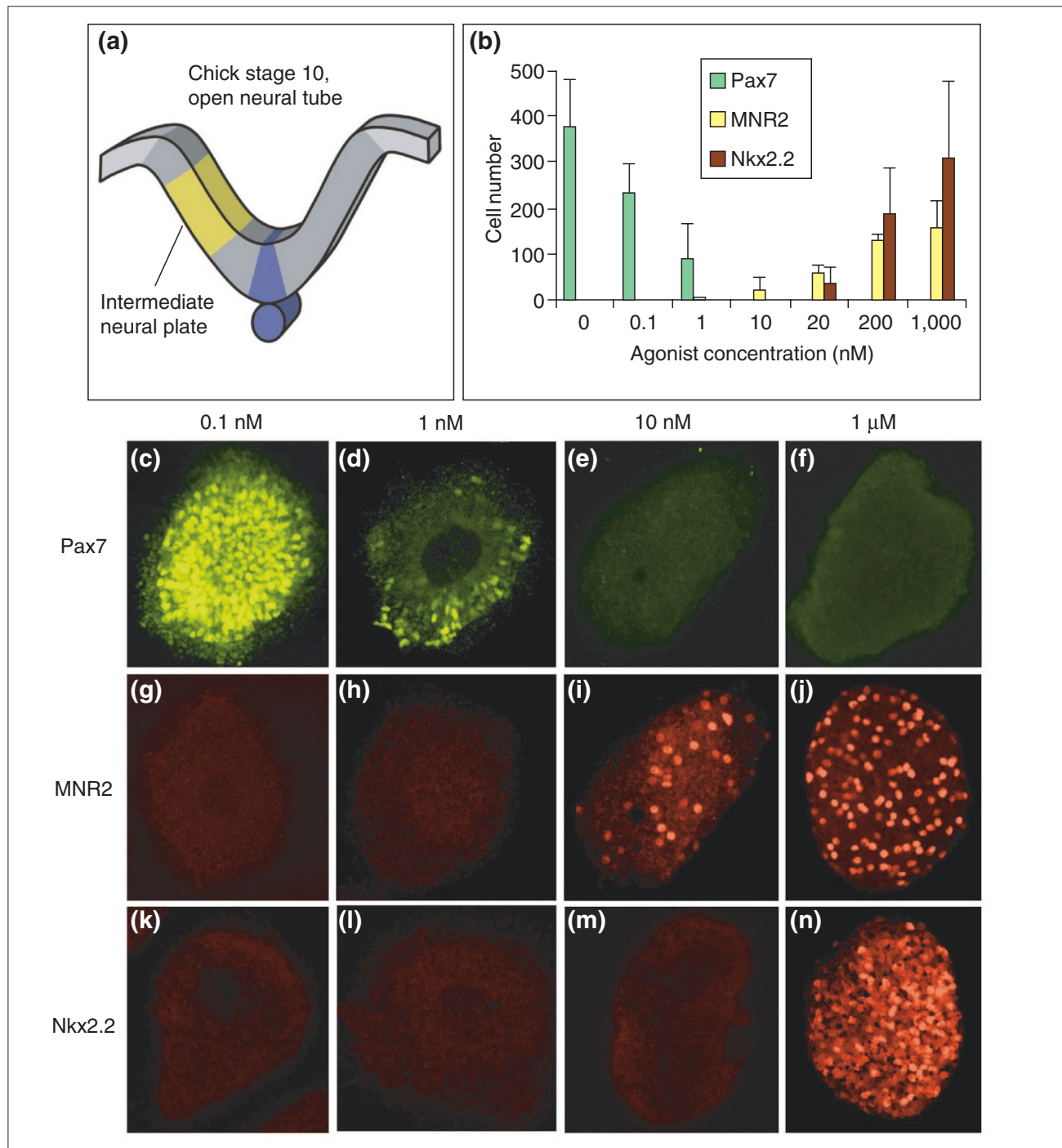
Figure 2

The concentration-dependent response to Hh agonist of neural progenitor markers in neural plate explants. **(a)** The intermediate region of neural plate was dissected from stage 10-11 chick embryos and cultured in the presence of varying concentrations of Hh-Ag 1.3 (agonist) for 22 hours. Explants were then immunostained for Pax7, MNR2 and Nkx2.2 and the number of immunoreactive cells per explant was counted. **(b)** The average number of immunoreactive cells per explant in response to increasing concentrations of Hh-Ag 1.3 (n = 6 explants). Error bars represent standard deviations. **(c-n)** Confocal images of representative explants cultured in the presence of different concentrations of the agonist and stained for (c-f) Pax7; (g-j) MNR2; and (k-n) Nkx2.2. Pax7 is expressed only at the lowest concentrations of the agonist (c,d), MNR2 at intermediate and high concentrations (i,j), and Nkx2.2 only at high concentrations of agonist (n).

*Ptc1^lacZ^* was greatly extended dorsally in the neural tube and throughout the adjacent mesoderm (Figure 3b,d). These embryos also displayed open rostral neural tubes, similar to those of *Ptc1^-/-^* embryos. These experiments demonstrate that the agonist compound effectively activates Hh signaling *in vivo* following oral administration.
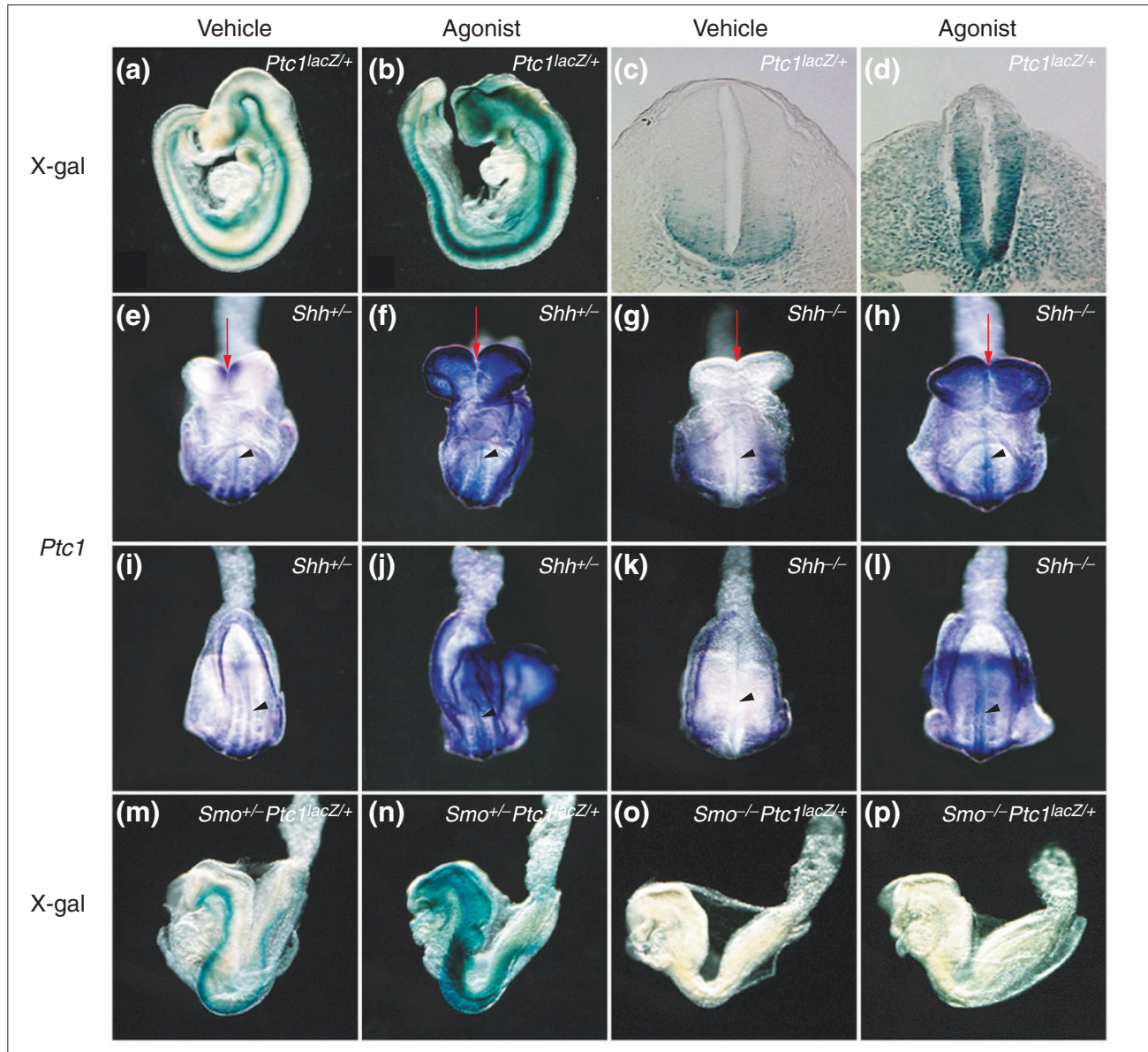

Figure 3
In vivo assays of an Hh agonist. (**a-d**) The Hh agonist Hh-Ag 1.2 up-regulates Hh signaling in mouse embryos *in utero*. Expression of *Ptc1^lacZ^* in E9.5 *Ptc1^lacZ/+^* embryos after treatment with vehicle (a,c) or Hh-Ag 1.2 (b,d). (a,b) Lateral views of whole embryos stained with X-gal; (c,d) transverse sections through E9.5 embryos following X-gal staining. *Ptc1* expression is dorsally expanded throughout the ventral neural tube and adjacent mesoderm in agonist-treated embryos (compare b,d with a,c). Note the open neural tube in the head of these embryos (b). (**e-p**) The agonist complements the loss of Shh but requires Smo to activate Hh signaling *in utero*. (e-l) Whole-mount *in situ* hybridization analyses of the expression of *Ptc1* gene in E8.5 embryos (n = 4); (e-h) ventral anterior views, and (i-l) ventral posterior views, of embryos heterozygous (e,f,i,j) or homozygous (g,h,k,l) for an *Shh*-null allele. (m-p) Lateral views of X-gal staining of *Ptc1^lacZ^* expression in E8.5 *Ptc1^lacZ/+^* embryos (n = 4) heterozygous (m,n) or homozygous (o,p) for a *Smo*-null allele. (e,g,i,k,m,o) Vehicle-treated embryos; (f,h,j,l,n,p) Hh-Ag 1.2- (agonist-) treated embryos. Red arrows in (e-h) indicate the partial rescue of midline structures in *Shh^-/-^* embryos (g) by agonist treatment (h). Black arrowheads in (e-l) indicate expression in the midline.

Agonist site of action in vivo

Having established an *in utero* assay for Hh signaling, we next investigated whether the agonist could rescue aspects of *Shh*- or *Smo*-mutant phenotypes, by monitoring *lacZ* expression in *Smo*^{-/-} *Ptc1*[lacZ/+] embryos [26] and *Ptc1* mRNA levels in *Shh*^{-/-} embryos.

Pregnant mice from *Shh*^{+/-} and *Smo*^{+/-} intercrosses were treated by oral gavage with vehicle or agonist (15 mg/kg) at 6.5 and 7.5 dpc. Embryos were collected at 6-8 somite stages (E8.5) when the midline defects are first detectable in both *Shh*^{-/-} and *Smo*^{-/-} embryos, but prior to any general retardation of growth and development [26,27]. In both *Shh*^{+/-} and *Smo*^{+/-} *Ptc1*[lacZ/+] embryos, *Ptc1* was detected in ventral neural tube, somites and lateral plate mesoderm (Figure 3e,i,m). Treatment with the agonist dramatically enhanced and expanded the expression of *Ptc1* in these heterozygous embryos (Figure 3f,j,n). This was consistent with what we have observed in wild-type embryos (Figure 3a-d). It is worth noting that the agonist-treated embryos exhibited overgrowth of the headfolds and hindbrain, reminiscent of *Ptc1*^{-/-} embryos (compare Figure 3e,m with f,n).

Shh^{-/-} and *Smo*^{-/-} embryos at this stage (6-8 somites) started to show fused ventral lips of the cephalic folds, and a single continuous optic vesicle, indicating lack of a clearly defined midline (red arrow, Figure 3g, and data not shown). As expected, *Ptc1* expression was not detected in the ventral neural tube of the vehicle-treated *Shh*^{-/-} embryos (arrowhead, Figure 3g), whereas expression was seen in lateral plate mesoderm and weakly in somites (Figure 3g,k). This is most likely due to Ihh signaling in these tissues [26]. Both Shh and Ihh signaling were dependent on Smo, however, because *Ptc1* expression could not be detected in *Smo*^{-/-} embryos (Figure 3o).

Following agonist treatment, we observed that the neural tube and somite expression of *Ptc1* in *Shh*^{-/-} embryos was greater than vehicle-treated wild-type levels (compare Figure 3h,l with e,i). The midline defects in *Shh*^{-/-} embryos were at least partly rescued by agonist treatment (compare Figure 3g and h; red arrows). Like *Shh*^{+/-} embryos, *Shh*^{-/-} embryos had overgrown headfolds after administration of the Hh agonist (Figure 3f and h). In contrast, agonist treatment had no detectable effect on either morphology or *Ptc1* expression in *Smo*^{-/-} embryos (compare Figure 3o and p). In summary, these studies demonstrate that agonist activity *in vivo* does not depend upon Shh, but that Smo is absolutely required.

Mechanism of action
Chemical epistasis studies
We sought to determine the level at which the agonist acts in the Hh pathway, in cultured cell assays. To begin addressing this question, we used the Hh reporter cell line to conduct competition experiments between the Hh agonist and known Hh- signaling antagonists that block the pathway at different levels (Figure 4a). These include: a Hh-protein-blocking antibody, 5E1 [23]; a natural product derivative, cyclopamine [9,10] that has recently been shown to act downstream of Ptc, perhaps at the level of Smo [11]; a recently identified synthetic small-molecule inhibitor, Cur61414, which has inhibitory properties similar to cyclopamine [17]; and forskolin, an adenylate cyclase/protein kinase A activator that is thought to block Hh signaling by stimulating degradation of members of the Gli family of transcriptional activators [2].

The Hh-blocking antibody 5E1 had no effect on pathway activation by the agonist (Figure 4b), while forskolin (Figure 4c), cyclopamine (Figure 4d) and Cur61414 (Figure 4e), were all inhibitory. The lack of inhibition by 5E1 eliminates the possibility that the small molecule agonist activates signaling indirectly via stimulation of Hh expression. Furthermore, this supports the data showing that the agonist can activate signaling in *Shh*^{-/-} embryos (Figure 3) and suggests that the agonist function is not only downstream of the Hh protein but also independent of the endogenous Hh-signaling modulators, Tout veloux and HIP, that act via the Hh ligand [2]. The competition experiment with forskolin showed identical inhibition curves for Hh protein and the agonist, strongly suggesting that the action of the small molecule is upstream of the protein-kinase-A-sensitive step in the pathway. In contrast, the competition experiments with cyclopamine (Figure 4d) and Cur61414 (Figure 4e) showed that Hh protein and the agonist differ in their sensitivity to these antagonists. Specifically, the agonist appears somewhat resistant to the inhibitory effect of cyclopamine and Cur61414. Identical results were seen using the slightly less active cyclopamine-related natural compound jervine, and the more potent synthetic derivative of cyclopamine, KAAD-cyclopamine (data not shown). These results argue that the agonist activates the pathway downstream of the Hh-Ptc interaction while cyclopamine, Cur61414 and the agonist may act at a similar level in the Hh-signaling cascade.

Regulation of Ptc and Smo by Hh protein and Hh agonist
Recent work in *Drosophila* tissue culture has shown that endogenous Ptc and Smo proteins are differentially affected by the addition of Hh to the growth medium [5]. Ptc was destabilized, while Smo accumulated following post-translational modification. To test whether similar phenomena occur in mammalian cells with Hh protein and agonist, we generated stable cell lines expressing two epitope-tagged proteins, Ptc coupled to green fluorescent protein, Ptc-GFP, and Smo coupled to a fragment of influenza hemagglutinin,
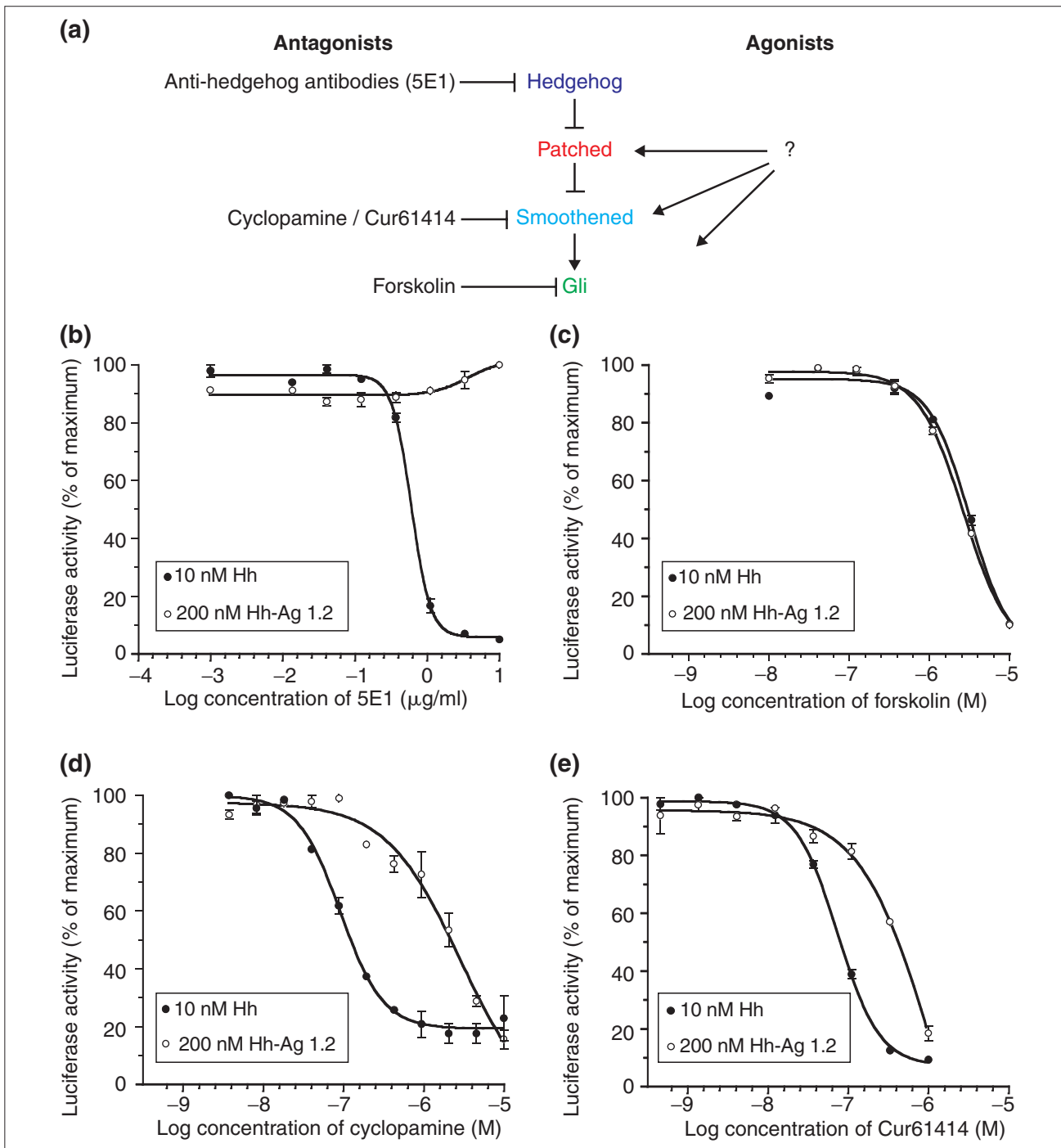
Figure 4

Analysis of the agonist's site of action, using characterized Hh-pathway antagonists. **(a)** The Hh-signaling pathway. The major components are shown, along with the suspected sites of action of four antagonists: 5E1, the Hh-ligand-binding/blocking monoclonal antibody; cyclopamine, the natural product inhibitor, activity of which maps downstream of Ptc; forskolin, the adenylate cyclase activator that functions via protein kinase A to activate destruction of Ci/Gli; and a recently identified Hh-signaling antagonist Cur61414. Lines with arrowheads represent activation and blunt-ended lines represent repression. **(b-e)** Luciferase-based reporter assays of Hh signaling showing inhibitory dose response on cells activated by Hh protein (10 nM) or Hh-Ag 1.2 (200 nM) of (b) 5E1; (c) forskolin; (d) cyclopamine; and (e) Cur61414. Data points represent the averages (n = 3) with standard deviations depicted by error bars.

HA-Smo. Figure 5a shows an immunoprecipitation (anti-GFP) plus protein blot (anti-Ptc) analysis of extracts from these cells treated for 4, 8 and 24 hours with vehicle, 25 nM Hh protein or 0.2 μM Hh agonist (see Figure 1e; Hh-Ag 1.2). This experiment shows that Ptc-GFP appears to be destabi-

lized by Hh protein but not by the agonist. Similar results were seen at higher doses of agonist (up to 2 μM) and in several independent lines (data not shown). These data further support the idea that Hh protein and the agonist act in distinct ways to stimulate the pathway.
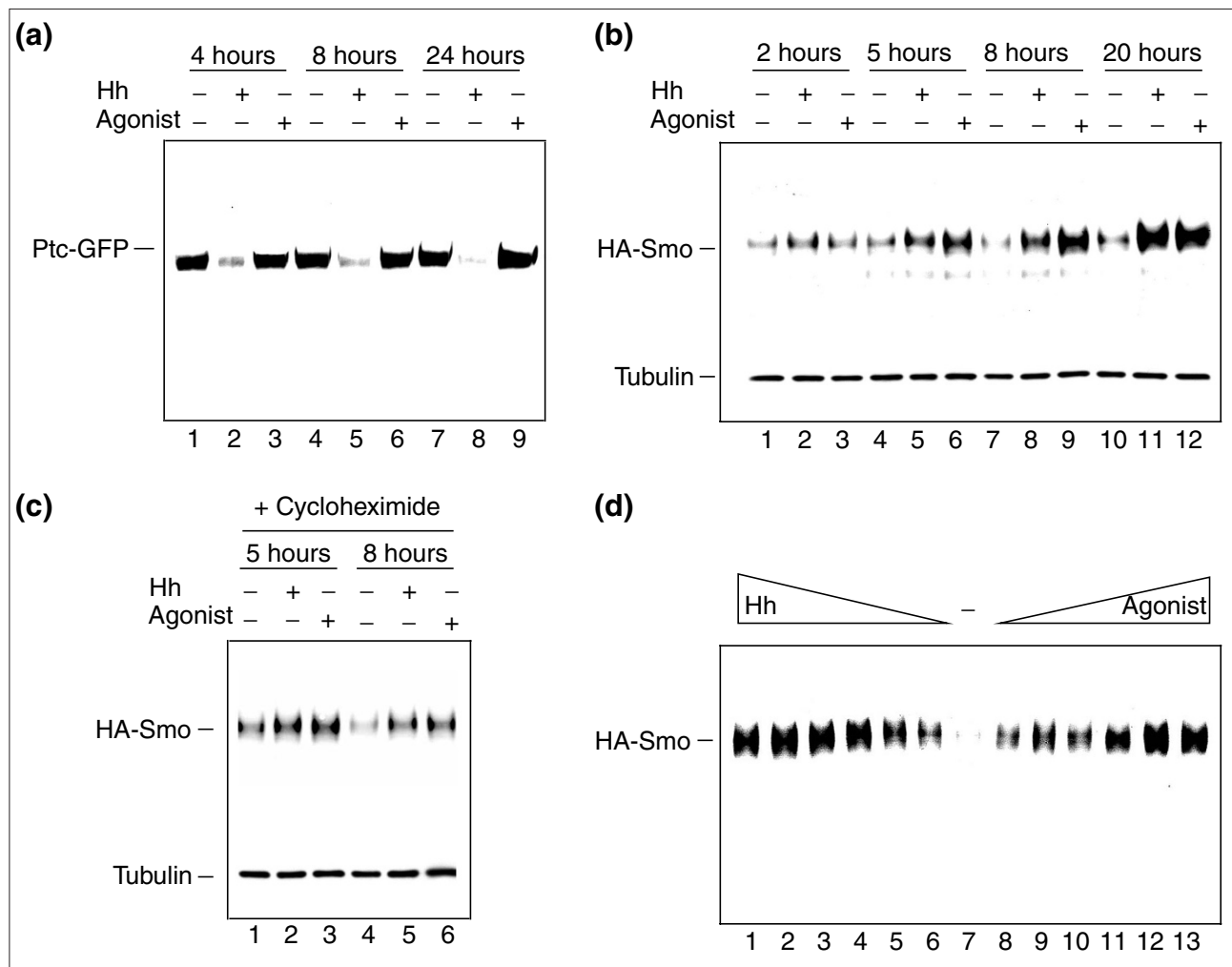

Figure 5
The effects of Hh protein and agonist on vertebrate Smo and Ptc proteins. A stable cell line expressing Ptc-GFP and HA-Smo retroviral constructs was generated to evaluate the effects of Hh protein versus agonist on the Hh receptor components. **(a)** Anti-Ptc protein blot of anti-GFP immunoprecipitates, fractionated by SDS-polyacrylamide gel electrophoresis, from cells treated with vehicle (lanes 1,4,7), 25 nM Hh protein (lanes 2,5,8) or 0.2 μM Hh-Ag 1.2 (agonist; lanes 3,6,9), for 4 hours (lanes 1-3), 8 hours (lanes 4-6) or 24 hours (lanes 7-9). **(b)** Anti-HA protein blot of cell extracts, fractionated by SDS-polyacrylamide gel electrophoresis, from cells treated with vehicle (lanes 1,4,7,10), 35 nM Hh protein (lanes 2,5,8,11) or 0.5 μM Hh-Ag 1.2 (agonist; lanes 3,6,9,12), for 2 hours (lanes 1-3), 5 hours (lanes 4-6), 8 hours (lanes 7-9) or 20 hours (lanes 10-12). **(c)** Anti-HA protein blot of cell extracts, fractionated by SDS-polyacrylamide gel electrophoresis, from cells treated with vehicle (lanes 1,4), 35 nM Hh protein (lanes 2,5), or 0.5 μM Hh-Ag 1.2 (agonist; lanes 3,6), for 5 hours (lanes 1-3) or 8 hours (lanes 4-6). Cells used in (c) were also treated with cycloheximide to block new protein synthesis. Blots in (b) and (c) were reprobed with anti-tubulin antibody as a sample loading control. **(d)** Anti-HA protein blot of cell extracts, fractionated by SDS-polyacrylamide gel electrophoresis, from cells treated with decreasing concentrations of Hh protein (lane 1, 100 nM; lane 2, 50 nM; lane 3, 25 nM; lane 4, 12.5 nM; lane 5, 6.25 nM; lane 6, 3.12 nM), or with vehicle (lane 7), or with increasing concentrations of Hh-Ag 1.2 (agonist; lane 8, 15 nM; lane 9, 31.25 nM; lane 10, 62.5 nM; lane 11, 250 nM; lane 12, 500 nM; lane 13, 1 μM) for 22 hours. All blots were visualized by autoradiography using anti-HRP (horse radish peroxidase) secondary antibodies and a chemiluminescence reagent kit (Amersham).

Figure 5b shows an immuno-blot (anti-HA) of total extracts from HA-Smo-expressing cells treated for 2, 5, 8 and 20 hours with vehicle, 35 nM Hh protein or 0.5 μM Hh agonist. In contrast to the results with Ptc-GFP, incubation of cells with both Hh protein and the small-molecule agonist resulted in the apparent accumulation of HA-Smo protein after 5 hours of incubation. To test whether the accumulation of HA-Smo in response to Hh protein or the agonist required protein synthesis, a similar study was performed in the presence of cycloheximide (Figure 5c). Under these conditions, HA-Smo accumulation was detectable 5 hours after addition of either Hh protein or the agonist (Figure 5c); this result argues that the effect of Hh protein and the agonist on HA-Smo levels does not require new protein synthesis. Finally, with increasing concentrations of Hh protein and the agonist there is a clear dose-dependent increase of HA-Smo levels (Figure 5d). These effects on epitope-tagged Smo protein were observed in multiple lines (data not shown). Taken together, these data suggest that Hh protein and the agonist share the ability to stabilize Smo, but only Hh protein can destabilize Ptc. Yet the agonist is fully capable of activating the full signaling pathway.

Testing Smo as the molecular target

Binding in whole cells

Our biochemistry experiments (above) show that the agonist modulates Smo levels, and thus may activate Hh signaling by directly binding Smo. To explore this possibility we tested whether a tritiated form of the agonist analog Hh-Ag 1.5 could form a complex with Smo, when Smo is transiently overexpressed in 293T cells. Figure 6a shows immuno-precipitable counts of extracts from cells incubated at 37°C for 2 hours with 5 nM [^{3}H]-Hh-Ag 1.5 either in the absence (columns 1-3) or presence of competitors (columns 4-9).

Immunocomplexes from untransfected control and β-adrenergic-receptor transfected cells did not contain significant counts (Figure 6a, columns 1, 2). Immunocomplexes derived from cells expressing Smo (Figure 6a, column 3) resulted in the recovery of approximately 40,000 of the 800,000 added counts, however. To test the specificity of this apparent Hh-Ag/Smo complex, cells were incubated with 5 μM (1000-fold molar excess) of unlabeled Hh Ag 1.5 or an unlabeled, signaling-inactive but structurally similar compound, an Hh-Ag 1.1 derivative that has a two-carbon linker in place of the cyclohexane ring (Figure 6a; Hh-Ag 1.5, column 4; Hh-Ag control, column 5). The addition of the unlabeled Hh-Ag 1.5, but not the inactive Hh-Ag 1.1 derivative agonist control, resulted in the complete absence of counts in the immunocomplex. These results suggest that a stable, specific interaction can form between Smo and the Hh agonist.

It has been shown that the Hh-pathway antagonists cyclopamine and Cur61414 block signaling in a Ptc-independent manner [11,17] and therefore may act directly on Smo. Having established a binding assay for a small-molecule agonist binding to Smo-expressing cells, we next tested whether the Hh antagonists could selectively compete out binding of [^{3}H]-Hh-Ag 1.5. To perform theses studies, Smo-overexpressing 293T cells were incubated for 2 hours at 37°C with 5 nM [^{3}H]-Hh-Ag 1.5 in the presence of either KAAD-cyclopamine at 5 μM (Figure 6a, column 6), the related but inactive plant compound tomatadine at 5 μM (Figure 6a; Antag control 1, column 7), Cur61414 at 5 μM (Figure 6a, column 8), or a related but inactive Cur61414 derivative (Figure 6a; Antag control 2, column 9) at 5 μM. These data show that the Hh-signaling inhibitors, but not structurally related inactive compounds, can significantly compete with the binding of the Hh agonist to Smo-expressing cells. This supports the model that all of these small-molecule modulators of Hh signaling are direct ligands of Smo.

We next asked whether a derivative of the Hh agonist carrying a photoactivatable crosslinker could be coupled directly to Smo, to facilitate further biochemical characterization of the binding site. To perform this experiment we synthesized a tritiated diazirine derivative of Hh-Ag 1.2 with an EC$_{50}$ in the cell-based assay of 35 nM (data not shown). We incubated this compound at 0.5 μM with HA-Smo- or control, GFP-transfected 293T cells and subsequently ultraviolet-irradiated them to initiate crosslinking. Fractionation by SDS-polyacrylamide gel electrophoresis and autoradiography of the resulting immunocomplexes from these cells showed crosslinking exclusively to HA-Smo, but with an efficiency of less than 1% (data not shown). This result demonstrates that a Hh-agonist derivative can be covalently crosslinked to Smo in living cells. More efficient crosslinkers are required to extend these studies, however.

Cell-free membrane-binding assays

To test whether the Hh agonist could interact with Smo *in vitro*, we transiently overexpressed murine Smo, murine Ptc, rat β2-adrenergic receptor and GFP in 293T cells, harvested membranes and performed a filtration membrane-binding assay in a 96-well plate with [^{3}H]-Hh-Ag 1.5 added at 2 nM. Figure 6b shows a bar graph of the bound counts from these binding assays (murine Smo, column 1; GFP, column 2; βAR, column 3; murine Ptc1, column 4; and a no-membrane plate control, column 5). The no-membrane control (column 5) was included to show the degree of non-specific binding to the filter-plate apparatus. The Smo-containing membranes (column 1) are the only samples that exhibit significant binding above that seen in the absence of membranes.

To assess the specificity of binding, we repeated the experiment in the presence and absence of a 1000-fold molar excess of unlabeled agonist (2 μM). The addition of 'cold' compound completely competed out these counts (Figure 6c, column 1 compared to column 2). To control for this observation, we added an unlabeled, inactive Hh agonist to the binding assay at 2 μM (a 1000-fold molar excess). This

compound was unable to compete out the binding of [^{3}H]-Hh-Ag 1.5 to the Smo-containing membranes (Figure 6c, column 3). These results argue that Smo and the agonist form a specific complex *in vitro*, as predicted by the whole cell/immunocomplex binding assay (Figure 6a).

Having established an *in vitro* binding assay for the Hh agonist to Smo, we next tested whether the Ptc-independent Hh antagonists could selectively compete with the interaction. Binding was assayed in the presence of KAAD-cyclopamine at 10 μM (Figure 6c, column 4), tomatadine at 10 μM (Figure 6c; Antag control 1, column 5), Cur61414 at 10 μM (Figure 6c, column 6), or the inactive Cur61414 derivative (Figure 6c; Antag control 2, column 7) at 10 μM. These data show that the Hh-signaling inhibitors, but not structurally related inactive compounds, can significantly compete with the binding of the Hh agonist to Smo membranes.

Kinetics, saturation and competition binding analysis

Next, we sought to generate association, dissociation and saturation-binding curves, in order to derive affinity
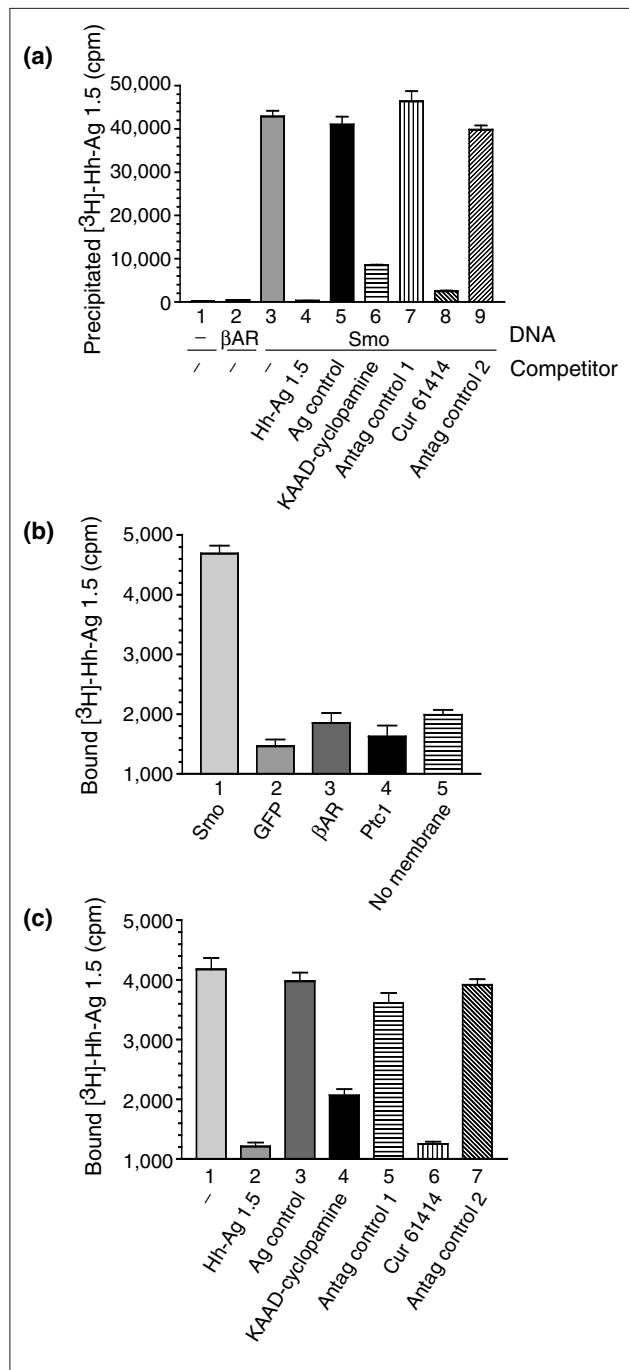

Figure 6

Assessing whether Smoothened is the molecular target of the Hh agonist. **(a)** The number of counts per minute (cpm) precipitated from an immunocomplex binding assay of 293T cells incubated with [^{3}H]-Hh-Ag 1.5. Anti-HA (columns 1,3-9) or anti-v5 (column 2) immunocomplexes were isolated from 293T cells that were untransfected (column 1) or transfected with expression constructs encoding a rat β2-adrenergic receptor cDNA carrying a v5 epitope tag (column 2; βAR), or an HA-epitope-tagged *Smo* cDNA (columns 3-9). Prior to cell lysis and immunoprecipitations, these cells were incubated with 5 nM [^{3}H]-Hh-Ag 1.5 alone (columns 1-3) or with 5 nM [^{3}H]-Hh-Ag 1.5 in the presence of 5 μM of various unlabeled compounds (columns 4-9): Hh-Ag 1.5 (column 4); an inactive Hh-Ag 1.1-derivative containing a two-carbon linker instead of the cyclohexane ring (Ag control, column 5); the potent natural product Hh-signaling-inhibitor derivative KAAD-cyclopamine (column 6); the inactive natural product tomatadine (Antag control 1, column 7); the synthetic Hh-signaling inhibitor Cur61414 (column 8); or an inactive derivative of Cur61414 (Antag control 2, column 9). Standard deviations (n = 2) are represented by error bars. **(b,c)** Filtration membrane-binding assay using [^{3}H]-Hh-Ag 1.5 (2 nM) and membranes (approximately 5 μg protein) from 293T cells transfected with different cDNA constructs. (b) Bound [^{3}H]-Hh-agonist (cpm) when using membranes from cells transfected with murine Smo (column 1); GFP (column 2); rat β2-adrenergic receptor (βAR, column 3); and murine Ptc1 (column 4). A no-membrane control (column 5) is also included, to demonstrate the level of nonspecific binding associated with the filtration plate apparatus. (c) A competition experiment using membranes from cells transfected with murine Smo and incubated with [^{3}H]-Hh-Ag 1.5 (2 nM) in the presence of various unlabeled compounds: no competitor (-, column 1); 2 μM unlabeled Hh-Ag 1.5 (column 2); 2 μM inactive Hh-Ag 1.1 derivative (Ag control, column 3); KAAD-cyclopamine (column 4); tomatadine (Antag control 1, column 5); Cur61414 (column 6); or an inactive derivative of Cur61414 (Antag control 2, column 7). Standard deviations (n = 4) are represented by error bars.

constants for the interaction of the Hh agonist and Smo. To control for nonspecific binding we used either Cur61414 or Hh-Ag 1.5 as unlabeled competitors. Similar results were generated if control membranes (from cells transfected with GFP, βAR, or Ptc) were used to define the non-specific level (data not shown).

First, we performed a kinetic analysis to establish the reversibility of the binding reaction and the approximate incubation time required for equilibrium binding studies. Association assays were performed at 37°C by combining 2 nM [³H]-Hh-Ag 1.5 with Smo-containing membranes for various times prior to harvesting and counting. Dissociation studies were initiated by adding 2 μM unlabeled Hh-Ag 1.5 after 2 hours of association. Samples were then incubated for 1-26 hours prior to harvesting and counting. Figure 7a shows the association and dissociation phases of agonist binding to Smo-containing membranes. Using the Prism GraphPad software, these data were fit to one-phase exponential association and decay curves, respectively, and gave an association t½ of approximately 1 hour and a dissociation t½ of approximately 10 hours. These results demonstrate that the binding of the agonist to Smo is reversible and that equilibrium binding will require binding reaction times of approximately 50 hours (five times the t½ of dissociation).

Next, we performed a saturation binding experiment. To establish total, nonspecific, and specific binding curves (Figure 7b), we added a range of [³H]-Hh-Ag 1.5 concentrations (0.01-3 nM) in the presence or absence of unlabeled Hh-Ag-1.5 at 2 μM. Identical results were seen if Cur61414 at 10 μM was used as the competitor (data not shown). On the basis of the binding kinetics, incubations were carried out for approximately 45 hours at 37°C, to allow for equilibrium to be reached. Using the Prism GraphPad software to perform non-linear regression analysis and curve fitting, we concluded that the data best fit a simple one-site binding model with a predicted K_d of 0.37 nM for Hh-Ag 1.5. This K_d is in general agreement with the EC_{50} values observed in the cell-based assay (0.37 nM as compared to 1 nM).

To further validate our binding results, we performed a competition assay using several agonist derivatives across a range of concentrations (0.01 nM to 1 μM). Figure 7c shows the competition curves for Hh-Ag 1.5, Hh-Ag 1.3, Hh-Ag 1.2, Hh-Ag 1.1, and the signaling-inactive Hh-Ag 1.1 derivative described above. With the exception of the inactive derivative, these compounds all compete out the binding of [³H]-Hh-Ag 1.5 (0.4 nM) to the Smo-containing membranes. These data are best fit to a single-binding-site competition model that predicts the following K_i values: Hh-Ag 1.5, 0.52 nM; Hh-Ag 1.3, 8.4 nM; Hh-Ag 1.2, 22 nM; and Hh-Ag 1.1, 96 nM. These K_i values are in general agreement

with the agonist EC_{50} values in cell culture for these compounds, with the exception that the Hh-Ag 1.1 compound is not as potent in signaling assays (EC_{50} 2 μM) as its K_i (96 nM) might predict. This suggests an uncoupling of binding and signaling for certain agonists. Although binding affinities and signaling efficacy can correspond for certain ligand/receptor complexes, exceptions often arise [28] because binding affinity does not necessarily measure the ability of a compound to induce an active receptor conformation. As a control for these binding studies, identical competition experiments were performed with membranes from cells transfected with GFP, or with the β-adrenergic receptor. No specific binding or apparent competition was seen under these conditions (data not shown).

We next compared binding of KAAD-cyclopamine, Cur61414 and Hh-Ag 1.5 to a constitutively active mutant of Smo (Smo^act) or to wild-type Smo (Smo^wt). The two Hh-signaling antagonists, KAAD-cyclopamine and Cur61414, have shown decreased potency on Smo^act-expressing cells, leading to the speculation that they may bind this mutant form of Smo less well than the wild-type form [11,17]. We sought to determine whether the Hh agonist binds Smo^act with a higher affinity, an observation seen with certain ligands and constitutively active mutants of GPCRs [29]. To perform this experiment, we isolated membranes from cells transfected with a cDNA construct encoding a tryptophan-to-leucine mutation at residue 539 (W539L) of murine Smo. This oncogenic mutation has been found in human basal cell carcinoma [3] and the correspondingly mutated protein is capable of ligand-independent activation of the Hh pathway in cell-culture assays [11]. A kinetic and saturation binding assay with Smo^act-containing membranes showed that this mutant protein binds the Hh agonist with an affinity identical to that of Smo^wt (data not shown).

Using Smo^act- and Smo^wt-containing membranes, we then performed competition binding studies by adding increasing concentrations of unlabeled Hh-Ag 1.5, KAAD-cyclopamine or Cur61414 in the presence of [³H]-Hh-Ag 1.5 (0.4 nM). These binding curves (Figure 7d) can be fit to a single-site competition model. Although the K_i for Hh-Ag 1.5 on Smo^act-containing membranes was essentially identical to that observed for Smo^wt-containing membranes (approximately 0.5 nM), the K_i values of the Hh antagonists were seven-fold higher on the Smo^act- compared to the Smo^wt- containing membranes for both KAAD-cyclopamine (38.3 nM versus 5.8 nM) and Cur61414 (309 nM versus 44 nM). These results strongly support the model, initially hypothesized for cyclopamine [11], that the reduced potency observed for Hh antagonists on Smo^act-expressing cells is directly due to a reduced affinity of the antagonist for the mutated Smo protein. The agonist, on the other hand,
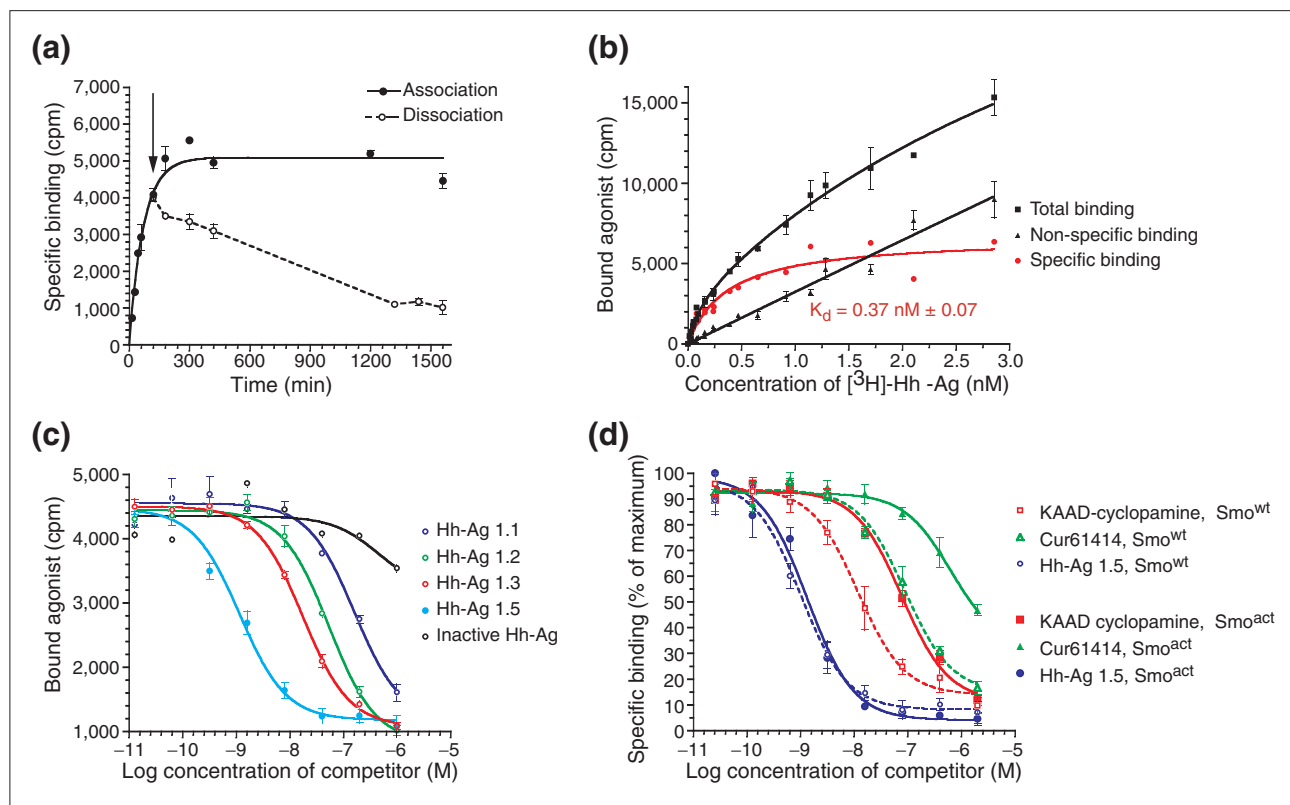
Figure 7
[³H]-Hh-agonist kinetic, saturation and competition binding analysis with Smo-containing membranes. **(a)** The association (solid line) and dissociation (broken line) time courses for the binding of [³H]-Hh-Ag 1.5 to membranes from Smo-overexpressing 293T cells. The arrow denotes the time at which 2 μM unlabeled [³H]-Hh-Ag 1.5 was added to initiate dissociation studies. **(b)** The total (squares), nonspecific (triangles) and specific (circles) binding (in cpm) of [³H]-Hh-Ag 1.5 to membranes from Smo-overexpressing 293T cells. Total and specific binding data were derived in the absence and presence of 2 μM unlabeled Hh-Ag 1.5, respectively. The specific curve (red) represents the difference between these curves. Similar specific curves resulted when control membranes or a no-membrane control plate was used to define the nonspecific binding, or if 10 μM Cur61414 was used as the competitor. A dissociation binding constant (K_d) of 0.37 nM is predicted from this single site binding isotherm. **(c)** A competition assay of [³H]-Hh-Ag 1.5/Smo binding by a set of agonist derivatives including Hh-Ag 1.5 , Hh-Ag 1.3, Hh-Ag 1.2, Hh-Ag 1.1, and an inactive Hh-agonist derivative. **(d)** A competition binding study showing the properties of the binding of KAAD-cyclopamine, Cur61414 and Hh-Ag 1.5 to wild-type Smo, Smo^{wt}, and a constitutively active Smo mutant protein, Smo^{act}, which contains an activating W539L amino-acid substitution. Competition curves on Smo^{wt} are shown by broken lines and the competition curves on Smo^{act} by solid lines. Standard deviations (n = 4) are represented by error bars for all data points.

would be predicted to bind to a site on Smo that is not affected by this gain-of-function Smo^{act} mutation.

Discussion

Hh signal transduction has been the focus of intense research over the past decade due to the central role it plays in development and its emerging biomedical relevance in areas ranging from regenerative medicine to oncology [2,30]. Our goal in these studies was to isolate and characterize small-molecule modulators of Hh signaling in order to understand better the regulation of pathway activation and to generate potential therapeutics. Our work shows

firstly that it is possible to identify potent small molecule agonists of Hh signaling, secondly that these compounds can mimic the effects of recombinant Hh protein in multiple assays used to define the properties of Hh signaling, thirdly that these compounds act by binding directly to Smo, and finally that two Ptc-independent inhibitors of Hh signaling compete for this binding to Smo, strongly suggesting they too act directly on Smo.

Models of Smo-ligand interaction

To interpret the results of the competition binding studies, we assume that the mutation in Smo^{act}, like those in constitutively activate mutants of other GPCRs [29], indirectly

influences ligand binding by creating a change in the normal equilibrium between the different conformations of Smo. Thus, the mutation would not directly influence the binding pocket for either ligand. A simple two-state model (Figure 8a) predicts that the agonist (Ag, green square) and the antagonist (Ant, pink circle) compete for the same site on Smo to activate or inactivate Hh-pathway signaling. It also suggests that antagonists should bind Smo^{act} with a lower affinity than they bind Smo^{wt}, while the agonist should bind with a higher affinity, as it prefers the active conformation. Such a model cannot accommodate our observations with the gain-of-function Smo mutant. Thus we introduce a ternary complex model (Figure 8b), used traditionally to describe the behavior of GPCRs in binding studies with agonist and antagonists [31], as well as constitutively active receptors [29]. The ternary complex model for Hh signaling suggests that there are two independent binding sites on Smo^{wt}, one specific for the agonist and another specific for antagonists. Binding at either site would decrease the affinity for interactions at the other site (allosteric binding with high negative cooperativity). The agonist-bound form represents the normal activated state, while the antagonist-bound form is considered the inactive conformation. There are also other conformations that would not be bound, or would be transiently bound, by both ligands. A signaling pathway coupler, or effector (in blue), is proposed to bind the activated state of Smo^{wt} so as to generate a complex competent to initiate Hh signaling. Throughout the discussion the term 'coupler/effector' is used to describe an unknown molecule that binds activated Smo in such a way as to trigger signal transduction. The model further suggests that the Smo^{act} protein resides in a stable conformation in the absence of agonist that is capable of forming an active coupler/effector complex resistant to antagonist, but not agonist, binding.

Specifically, our data suggest that the agonist binds and stabilizes (or induces) an active signaling state of Smo while the antagonists bind and stabilize (or induce) an inactive form. Furthermore, the gain-of-function Smo mutation renders the protein less sensitive to the inhibitors, presumably because the amino-acid substitution directly stabilizes or induces an active conformation. On the basis of a simple two-state model, one might predict an increased affinity of the agonist for the mutant form, but in our studies binding of the agonist, unlike the antagonist, is not affected by the activating mutation, suggesting that a more complex model requiring two binding sites and perhaps multiple active conformations is needed to account for the observations. Thus, we propose a variation of the classic 'ternary complex model' (Figure 8), a decades-old paradigm that has provided the foundation

for describing ligand induced conformational changes of GPCRs [31].

Briefly, if this model is applied to Hh signaling, it proposes that, firstly, agonist and antagonists act at independent sites to select active and inactive conformations of Smo; secondly, that Smo engages an undefined coupler/effector, when it is in its signaling state; and finally, that the gain-of-function mutant form of Smo, Smo^{act}, adopts an abnormal conformation that resembles the coupler/effector-bound signaling state of Smo with low affinity for antagonists but normal affinity for the agonist.

Activating Hh signaling through the GPCR-like Smo receptor

As a receptor class, GPCRs are considered excellent drug targets because they are often regulated through interactions with small natural ligands [32,33]. Specifically, studies of classic GPCRs, such as the β-adrenergic receptors, show that in the absence of endogenous ligand (agonists) these receptors exist in multiple interconvertible conformations that are predominately inactive [34]. Upon exposure to their natural ligands, however, the active receptor forms are preferentially stabilized, allowing them to readily engage G-protein couplers and to create signaling-competent complexes. Multiple compound classes have been isolated on the basis of their ability to compete for the binding of β-adrenergic receptors by their natural ligands. These competitors can mimic the natural ligand activity (agonists) or interfere with it (antagonists).

In addition to the binding sites for natural or endogenous agonists (orthosteric sites), many GPCRs have also been found to have allosteric sites [35]. These sites can bind natural ligands, as in the case of Zn ions and heparin for the dopamine and neurokinin receptors, respectively, or bind synthetic drugs such gallamine, in the case of the muscarinic receptors [35]. Binding of small molecules to these allosteric sites can modulate activity of a receptor without directly mimicking or competing out the interaction of ligands to the orthosteric sites. In summary, GPCRs have an array of potential regulatory binding sites, or potential drug targets.

How does Smo compare with other GPCRs with regard to the properties described above? Although there is clear structural homology between Smo and other GPCRs, endogenous ligands have yet to be discovered. Early models of Hh signaling proposed a Hh-regulated Ptc-Smo complex that directly controlled the conformation of Smo, making endogenous ligands unnecessary. But recent studies argue against this stoichiometric model [5,36], indicating that perhaps natural ligands should be considered. Furthermore,
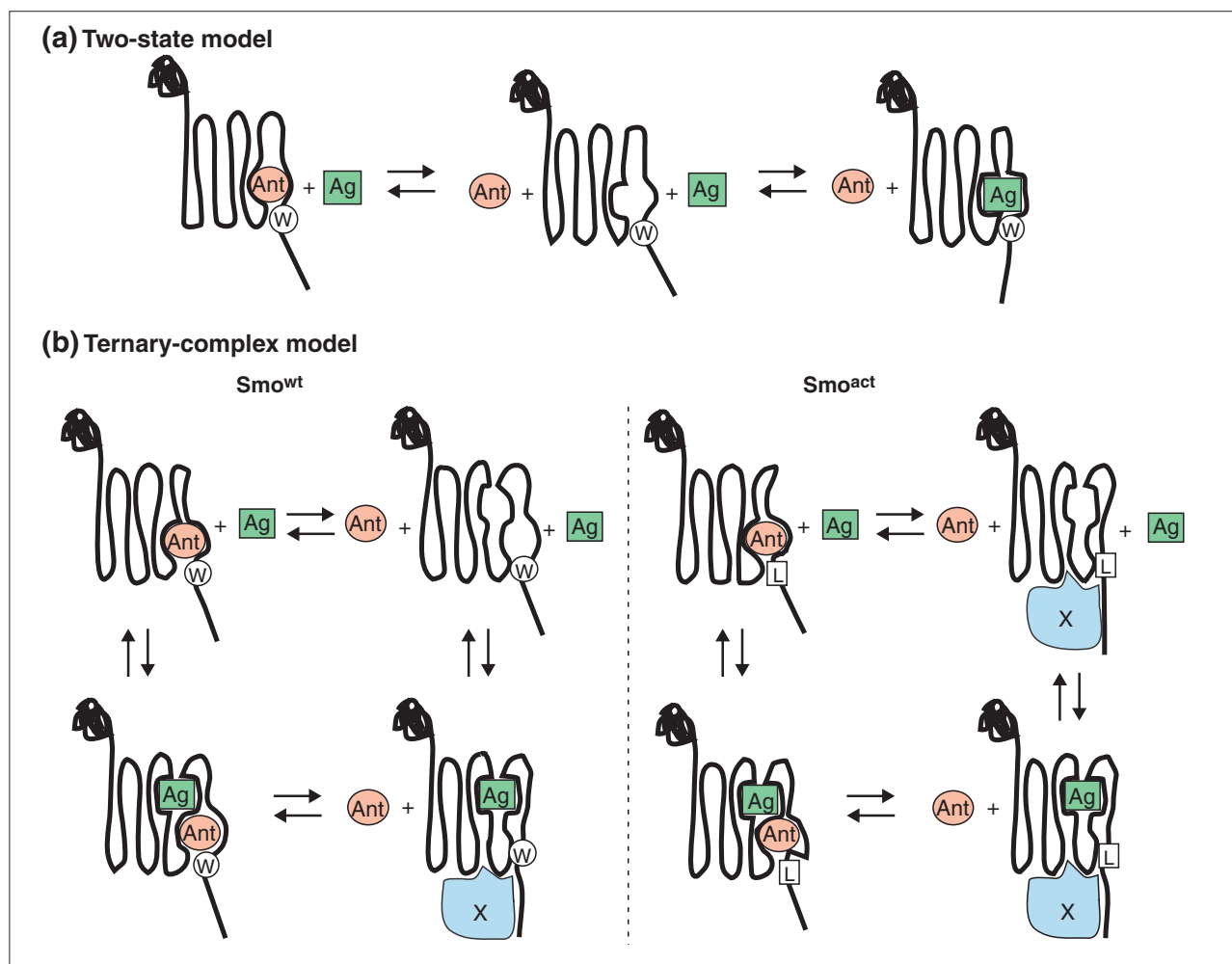
Figure 8
Models of small-molecule modulators binding to Smo. **(a)** The two-state model shows direct competition for a single binding site between the agonist (Ag, green square) and the antagonist (Ant, pink circle). **(b)** The ternary complex model suggests that there are two independent sites, and that agonist and antagonists are in a dynamic equilibrium (denoted by arrows) between Smo conformers bound at one site, both sites or not bound by ligand. On the basis of experimental data, binding at either site would decrease the affinity of interaction at the other site (allosteric binding with high negative cooperativity). A hypothetical signal transduction coupler, or effector, (the blue structure labeled X) is introduced in the ternary complex model. A coupler/effector-bound form is considered to be the active signaling complex. According to the model, only single active agonist-bound species of Smo[wt] is seen (bottom left). For Smo[act] (bottom right), the model predicts that the activating point mutation, W539L, results in a stable, distorted form of Smo that binds the antagonist poorly and has an increased affinity for the coupler/effector, even in the absence of agonist, thus leading to elevated basal signaling. This mutant form can nevertheless bind agonist and assume a conformation like that of the normal activated Smo[wt]. Residue 539 is designated as either W for Smo[wt] or as L in the Smo[act] mutant.

regarding G-protein-effector coupling for Smo, the results are also equivocal. Although no compelling data have been presented that directly link classic G-protein activation [37] to the canonical Hh pathway involving Ci/Gli stimulation [2], recent studies show that under certain conditions Smo can engage G-protein subunits in a Ptc-dependent manner [38] and that G-protein-mediated cAMP modulation may underlie certain effects of Hh on neuronal tissue [39].

Finally, with respect to pharmacological properties, our studies indicate that Smo behaves like a classic GPCR in many regards and that the models used to describe this large family of receptors can be applied to Hh signaling (Figure 8). Two relatively novel concepts for Hh signaling are raised by these GPCR models: firstly, the importance of considering the active Smo-coupler/effector complexes when modeling pathway regulation, and secondly the

potential for endogenous ligands in the regulation of Smo activity.

GPCR models for Smo and potential mechanisms of Ptc function

A recent study in *Drosophila* suggested that Hh stimulates the pathway via Ptc degradation and, as a result, Smo is stabilized through extensive phosphorylation at the plasma membrane where it initiates signaling [5]. This led to speculation that a Ptc-regulated phosphatase may control the subcellular distribution and stability of Smo [5]. Although suggestive, the studies in *Drosophila* did not establish that phosphorylation, translocation or stabilization of Smo is required for pathway stimulation. It is plausible that some or all of these effects on Smo result from a feedback inhibition mechanism that targets the activated Smo receptor. Interestingly, while we did observe stabilization of Smo by Hh in our mammalian cell experiments (Figure 5), we did not detect Smo phosphorylation or translocation to the plasma membrane (data not shown). Perhaps the cellular (or species) context dictates the degree to which the active conformations of Smo are associated with such changes. Thus, in considering models of Ptc function based on Hh-stimulated effects it is important to consider whether the form of Smo that is being observed is the active (coupler/effector bound) signaling state, or perhaps a downregulated and inactive form.

Several potential points for regulation by Ptc during the formation of a Smo-coupler/effector complex are apparent in a ternary complex model. The ideas proposed for the *Drosophila* system, in which Ptc may affect the levels of Smo or its subcellular localization, are easily accommodated. Ptc-induced instability of Smo protein would indirectly reduce the concentration of an active Smo-coupler/effector complex. Furthermore, limiting access of Smo to its effector through targeted vesicle trafficking would prevent a signaling-competent complex from forming. Alternatively, Ptc could more directly maintain Smo in an inactive state. On the basis of our studies it is tempting to speculate that native small molecules with properties similar to our agonist and antagonists act directly on Smo in a Ptc-dependent manner. These putative endogenous Smo modulators could represent orthosteric or allosteric ligands.

The simplest model would have Ptc acting catalytically to dock a natural antagonist directly onto (or remove an agonist from) Smo. A more complex model would involve Ptc restricting the distribution of Smo such that it is forced into compartments containing the natural antagonists or lacking the natural agonists. Finally, Ptc could control the distribution of the endogenous small-molecule modulators themselves. Ptc shares sequence homology with molecules

associated with vesicle trafficking and transporter activity, namely SCAP and NPC1 [36,40-42]; if it also shares the activities of these molecules, as suggested by a recent study [36], then the possibility of the existence of endogenous Smo ligands that are docked via Ptc should be explored.

Therapeutic potential of a Hh-pathway agonist

Various studies in mammals have shown that *Hh* genes are expressed in discrete areas of the adult organism and may function in the normal maintenance of mature organ systems [43-46]. In addition, the regenerative healing of vascular and skeletal tissues following acute injuries appears to be aided by re-activating the Hh-signaling cascade [47,48]. Taken together, these observations suggest that the Hh pathway may represent a point of intervention for treating certain degenerative disorders. Two recent studies in models of Parkinson's disease and peripheral nerve damage support this claim, by demonstrating that pathway activation with a Hh-protein ligand has therapeutic value [49,50]. On the basis of our current understanding of these models and the specific mechanism of action of the Hh agonists, we predict that an agonist-derivative with low toxicity and favorable pharmacokinetics would replicate these positive results. As a drug, a Hh agonist would represent an attractive alternative to an expensive Hh-protein therapeutic. Beyond the economics, for disorders of the central nervous system a small molecule with the potential to cross the blood-brain barrier would eliminate the need for injections directly into the brain, the current delivery mode for central nervous system protein therapies.

Materials and methods
Chemical libraries and medicinal chemistry
The compound libraries used in our screens were purchased from a number of commercial vendors and were primarily generated by combinatorial chemistry approaches. The Hh-agonist class was isolated from a library synthesized by Oxford Asymmetry International, now EvotecOAI. The derivatization of this compound class utilized standard procedures, the details of which will be published elsewhere.

Cultured cell line assays
TM3 and C3H10T1/2 cells (ATCC; Manassas, USA) were maintained according to the instructions of ATCC. Stable Hh-signaling reporter cell lines were established by G418 selection following transfection with a luciferase reporter plasmid [20] containing the neomycin-resistance gene. Hh signaling was monitored by plating cells at 70% confluence in growth medium. After 24 hours the cells were changed to 0.5% serum-containing medium, and Hh protein or compounds were added; 24 hours later the cells were either monitored for luciferase activity using the Luc-lite assay kit

(Packard Instrument Company, Meriden, USA) or harvested for RNA isolation using an RNA isolation kit (Qiagen; Valencia, USA). RNA was subjected to quantitative RT-PCR analysis (Taqman; Applied Biosystems, Foster City, USA) utilizing *Gli1*, *Ptc1* and *GAPDH* primers and probes. Assays were run on a Prism 7700 instrument (ABI; Applied Biosystems).

Recombinant Hh protein
The Hh protein used in the studies described here was bacterially overexpressed amino-terminal human Shh modified at its amino-terminal cysteine by an octyl maleimide moiety [21]. This lipophilic Shh form showed comparable potency to native Shh in the cell-based reporter assay (data not shown).

Retroviral cell lines
Mouse *Smo* and *Ptc1* genes were introduced by a retroviral approach utilizing the pLPCX vector (Clontech; Palo Alto, USA) to limit the copy number per cell. Stable HA-Smo and Ptc-GFP lines were established by puromycin selection following infection of TM3 cells with the respective retroviruses. TM3 cells expressing both epitope-tagged Ptc and Smo were derived by infecting first with an HA-Smo construct and subsequently with a Ptc-GFP construct. The levels of Ptc were relatively low in these lines and a standard immunoprecipitation procedure followed by western blotting was required to detect the Ptc-GFP protein. The HA-Smo protein was highly expressed and was easily detected in western blots of whole cell extracts. The HA tag was subcloned into the *Smo* gene so that it would reside immediately after the Smo signal sequence. The GFP tag was inserted before the stop codon of the *Ptc* open reading frame.

In utero Hh-signaling assays
Generation of *Ptc1^lacZ^*, *Shh* and *Smo* mutant mice has been described previously [25,26]. *Ptc1^lacZ/+^* mice were kindly provided by Matthew Scott. *Shh^+/-^* and *Smo^+/-^* mice were kindly provided by Andrew McMahon. Agonist solution was prepared in fine suspension in 0.5% methylcellulose/0.2% Tween 80 at 1.5 mg/ml. Compound was administered by oral gavage to pregnant mice once a day for two days at 100 µl per 10 g body weight. Embryos were collected 24 hours later. Whole-mount *in situ* hybridization with *Ptc1* probe and X-gal staining for whole-mount β-galactosidase detection were performed as described [26]. For histology, embryos stained with X-gal were post-fixed in 4% paraformaldehyde, wax-embedded, and 20 µm sections were prepared.

Primary cerebellar cultures
Cerebellar neurons were dissected out of postnatal (one week) rat brains, and placed into primary cell culture. Briefly, cells were placed in 96-well plates at a density of approximately 150,000 cells per well in basal medium of Eagle (Gibco; Carlsbad, USA) supplemented with 26 mM KCl, 2 mM glutamine and 10% calf serum. Treatment agents were added once, on the first day of culture (0 DIV). Cells were left in culture until 2 DIV, when [³H]-thymidine was added for 5 hours. Cells were then lysed, and the incorporation of [³H]-thymidine was determined by scintillation counting.

Neural plate explant assay
Intermediate regions of the open neural tube (i-explants) were dissected from stage 10-11 chick embryos and embedded in collagen gel [23]. Explants were cultured in Ham-F12 supplemented with 3 g/l D-glucose, Mito Serum Extender (Collaborative Research; Bedford, USA), penicillin/streptomycin (Gibco), 2 mM L-glutamine (Gibco) and Hh-Ag 1.3 (0.1, 1, 10, 20, 200 and 1000 nM prepared as 1000X stocks in DMSO; n = 6 explants). As a control, some explants were cultured with vehicle alone or with octylated Hh-N recombinant protein. Cultures were fixed after 22 hours, stained with mouse monoclonal antibodies against Pax7, MNR2 or rabbit polyclonal antibodies against Nkx2.2 and the number of immunoreactive cells per explant counted.

Whole cell/immunocomplex binding assay
Cultured cells - 70% confluent 293T cells in 6-well plates - were either left untransfected or transfected using Fugene6 with a pCDNA3.1 construct containing HA-tagged Smo or v5-epitope tagged β2AR (Invitrogen; Carlsbad, USA). After 48 hours cells were switched from 10% fetal bovine serum containing DME media to 0.5% FBS containing media supplemented with either 5 nM [³H]-Hh-Ag 1.5 alone or 5 nM [³H]-agonist plus 5 µM of various competitors (see Results). After 2 hours of incubation at 37°C, cells were washed one time with PBS and subsequently lysed in 0.5 ml of lysis/wash buffer containing 1% NP40 in Tris-buffered saline plus an EDTA-free protease inhibitor cocktail (Roche; Indianapolis, USA) for 20 minutes at 4°C. Cell extracts were spun at 14,000 rpm in a microcentrifuge and supernatants were incubated for 40-60 minutes with either anti-HA beads (Roche) or anti-v5 antibody (Invitrogen) and Protein A beads (Pierce; Rockford, USA) to form immunocomplexes. Immunobeads were then spun down and washed three times with 0.5 ml lysis/wash buffer per wash. The washed pellets were then resuspended in SDS sample buffer and combined with scintillation fluid. Counts per minute (cpm) for each sample were then determined in a scintillation counter (Packard topcount).

Membrane binding assays
Membranes were prepared as follows. Briefly, approximately 10⁸ cells were transfected with pcDNA 3.1 constructs (Invitrogen) bearing either murine *Smo* (wild-type or

W539L mutant), GFP, rat β2AR (Invitrogen), or murine *Ptc* cDNAs using Fugene 6 (Roche). After 48 hours cells were harvested by scraping in PBS, centrifuged at 1,000 x *g* for 10 minutes, and gently resuspended in around 10 ml of a 50 mM Tris pH 7.5, 250 mM sucrose buffer containing an EDTA-free protease inhibitor cocktail (Roche). This cell suspension was then placed in a nitrogen cavitation device (Parr Instrument Co, Moline, USA) and exposed to nitrogen gas (230 psi) for 10 minutes. Lysed cells were released from the device and centrifuged at 20,000 rpm in an SS34 rotor for 20 minutes at 4°C. Supernatants were discarded and the pellets were resuspended in 10% sucrose, 50 mM Tris pH 7.5, 5 mM MgCl, 1 mM EDTA solution using three 10-second pulses with a Polytron (Brinkman; Westbury, USA) at a power setting of 12. Using these membranes, filtration binding assays were performed according to previously described protocols [28]. To reduce nonspecific binding, 96-well filtration plates (fiberglass FB filters; Millipore, Bedford, USA) were pre-coated as suggested by the manufacturer with 0.5% polyethyleneimine + 0.1% BSA and then washed four times with 0.1% BSA.

For association and dissociation studies, membranes (1.5 µg total protein) were incubated in polypropylene tubes with 2 nM [^{3}H]-Hh-Ag 1.5 in the presence or absence of 2 µM competitor in binding buffer (50 mM Tris pH 7.5, 5 mM MgCl, 1 mM EDTA, 0.1 % bovine serum albumin) plus EDTA-free protease inhibitor cocktail (Roche) in a final volume of 250 µl for 1-26 hours at 37°C. For saturation and competition binding analysis, membranes (1.5 µg total protein) were incubated on the plates with various concentrations of the [^{3}H]-Hh-Ag 1.5 (plus and minus competitors) in binding buffer plus EDTA-free protease inhibitor cocktail (Roche) at a final volume of 1 ml for approximately 45 hours at 37°C to allow binding to reach apparent equilibrium. Binding reaction mixtures (0.2 ml for association/dissociation studies and 0.75 ml in saturation and competition experiments) were then transferred to the pre-coated 96-well filtration plates (Millipore fiberglass FB filters), filtered and washed over a vacuum manifold with six 300 µl per well washes of binding buffer supplemented with 2% hydoxypropyl cyclodextrin (HPCD; Sigma; ST Louis, USA) + 0.1% BSA to decrease non-specific binding. Identical results were obtained if incubations were done in borosilicate glass or siliconized plastic tubes. Centrifugation assays were also performed that replicate the filtration assay results (data not shown). Additionally, these experiments showed that the extent of ligand depletion was less than 10% in these studies. Binding-kinetics experiments were performed similarly to the saturation and competition studies. All binding data were evaluated using a nonlinear regression analysis program (Prism; GraphPad; San Diego, USA). K_i values were calculated using the Cheng-Prusoff correction equation [28], where $K_i = IC_{50}/1+[L]/K_d$, and K_d for Hh-Ag 1.5 was determined to be 0.37 nM by the saturation analysis.

Note added in proof
Related results demonstrating the action of cyclopamine on Smo have been reported by Beachy and colleagues [51,52].

References
1. Nusslein-Volhard C, Wieschaus E: **Mutations affecting segment number and polarity in *Drosophila*.** *Nature* 1980, **287:**795-801.
2. Ingham PW, McMahon AP: **Hedgehog signaling in animal development: paradigms and principles.** *Genes Dev* 2001, **15:**3059-3087.
3. Xie J, Murone M, Luoh SM, Ryan A, Gu Q, Zhang C, Bonifas JM, Lam CW, Hynes M, Goddard A, *et al.*: **Activating Smoothened mutations in sporadic basal-cell carcinoma.** *Nature* 1998, **391:**90-92.
4. Stone DM, Hynes M, Armanini M, Swanson TA, Gu Q, Johnson RL, Scott MP, Pennica D, Goddard A, Phillips H, *et al.*: **The tumour-suppressor gene *patched* encodes a candidate receptor for Sonic hedgehog.** *Nature* 1996, **384:**129-134.
5. Denef N, Neubuser D, Perez L, Cohen SM: **Hedgehog induces opposite changes in turnover and subcellular localization of patched and smoothened.** *Cell* 2000, **102:**521-531.
6. Cuenda A, Alessi DR: **Use of kinase inhibitors to dissect signaling pathways.** *Methods Mol Biol* 2000, **99:**161-175.
7. Sebolt-Leopold JS: **Development of anticancer drugs targeting the MAP kinase pathway.** *Oncogene* 2000, **19:**6594-6599.
8. Lee JC, Kassis S, Kumar S, Badger A, Adams JL: **p38 mitogen-activated protein kinase inhibitors - mechanisms and therapeutic potentials.** *Pharmacol Ther* 1999, **82:**389-397.
9. Cooper MK, Porter JA, Young KE, Beachy PA: **Teratogen-mediated inhibition of target tissue response to Shh signaling.** *Science* 1998, **280:**1603-1607.
10. Incardona JP, Gaffield W, Kapur RP, Roelink H: **The teratogenic *Veratrum* alkaloid cyclopamine inhibits sonic hedgehog signal transduction.** *Development* 1998, **125:**3553-3562.
11. Taipale J, Chen JK, Cooper MK, Wang B, Mann RK, Milenkovic L, Scott MP, Beachy PA: **Effects of oncogenic mutations in Smoothened and Patched can be reversed by cyclopamine.** *Nature* 2000, **406:**1005-1009.
12. Tekki-Kessaris N, Woodruff R, Hall AC, Gaffield W, Kimura S, Stiles CD, Rowitch DH, Richardson WD: **Hedgehog-dependent oligodendrocyte lineage specification in the telencephalon.** *Development* 2001, **128:**2545-2554.
13. van den Brink GR, Hardwick JC, Tytgat GN, Brink MA, Ten Kate FJ, Van Deventer SJ, Peppelenbosch MP: **Sonic hedgehog regulates gastric gland morphogenesis in man and mouse.** *Gastroenterology* 2001, **121:**317-328.
14. Kim SK, Melton DA: **Pancreas development is promoted by cyclopamine, a hedgehog signaling inhibitor.** *Proc Natl Acad Sci USA* 1998, **95:**13036-13041.
15. Chiang C, Swan RZ, Grachtchouk M, Bolinger M, Litingtung Y, Robertson EK, Cooper MK, Gaffield W, Westphal H, Beachy PA,

Dlugosz AA: **Essential role for Sonic hedgehog during hair follicle morphogenesis.** *Dev Biol* 1999, **205:**1-9.

16. Sukegawa A, Narita T, Kameda T, Saitoh K, Nohno T, Iba H, Yasugi S, Fukuda K: **The concentric structure of the developing gut is regulated by Sonic hedgehog derived from endodermal epithelium.** *Development* 2000, **127:**1971-1980.

17. Williams JA, Guicherit OM, Zaharian BI, Xu Y, Chai L, Gatchalian C, Porter JA, Rubin LL, Wang FY: **Identification of novel inhibitors of the hedgehog signaling pathway: Effects on basal cell carcinoma-like lesions.** *Proc Natl Acad Sci USA*, in press.

18. Tian SS, Lamb P, King AG, Miller SG, Kessler L, Luengo JI, Averill L, Johnson RK, Gleason JG, Pelus LM, *et al.*: **A small, nonpeptidyl mimic of granulocyte colony-stimulating factor.** *Science* 1998, **281:**257-259.

19. Zhang B, Salituro G, Szalkowski D, Li Z, Zhang Y, Royo I, Vilella D, Diez MT, Pelaez F, Ruby C, *et al.*: **Discovery of a small molecule insulin mimetic with antidiabetic activity in mice.** *Science* 1999, **284:**974-977.

20. Sasaki H, Hui C, Nakafuku M, Kondoh H: **A binding site for Gli proteins is essential for HNF-3beta floor plate enhancer activity in transgenics and can respond to Shh** *in vitro.* *Development* 1997, **124:**1313-1322.

21. Taylor FR, Wen D, Garber EA, Carmillo AN, Baker DP, Arduini RM, Williams KP, Weinreb PH, Rayhorn P, Hronowski X, *et al.*: **Enhanced potency of human Sonic hedgehog by hydrophobic modification.** *Biochemistry* 2001, **40:**4359-4371.

22. Ericson J, Rashbass P, Schedl A, Brenner-Morton S, Kawakami A, van Heyningen V, Jessell TM, Briscoe J: **Pax6 controls progenitor cell identity and neuronal fate in response to graded Shh signaling.** *Cell* 1997, **90:**169-180.

23. Ericson J, Morton S, Kawakami A, Roelink H, Jessell TM: **Two critical periods of Sonic Hedgehog signaling required for the specification of motor neuron identity.** *Cell* 1996, **87:**661-673.

24. Tanabe Y, William C, Jessell TM: **Specification of motor neuron identity by the MNR2 homeodomain protein.** *Cell* 1998, **95:**67-80.

25. Goodrich LV, Milenkovic L, Higgins KM, Scott MP: **Altered neural cell fates and medulloblastoma in mouse patched mutants.** *Science* 1997, **277:**1109-1113.

26. Zhang XM, Ramalho-Santos M, McMahon AP: **Smoothened mutants reveal redundant roles for Shh and Ihh signaling including regulation of L/R asymmetry by the mouse node.** *Cell* 2001, **105:**781-792.

27. Chiang C, Litingtung Y, Lee E, Young KE, Corden, JL, Westphal H, Beachy PA: **Cyclopia and defective axial patterning in mice lacking Sonic hedgehog gene function.** *Nature* 1996, **383:**407-413.

28. Enna SJ, Williams M, Ferkany JW, Kenakin T, Porsolt RD, Sullivan, JP (eds.): *Current Protocols in Pharmacology.* New York: John Wiley and Sons; 2000.

29. Samama P, Cotecchia S, Costa T, Lefkowitz RJ: **A mutation-induced activated state of the beta 2-adrenergic receptor. Extending the ternary complex model.** *J Biol Chem* 1993, **268:**4625-4636.

30. Taipale J, Beachy PA: **The Hedgehog and Wnt signalling pathways in cancer.** *Nature* 2001, **411:**349-354.

31. De Lean A, Stadel JM, Lefkowitz RJ: **A ternary complex model explains the agonist-specific binding properties of the adenylate cyclase-coupled beta-adrenergic receptor.** *J Biol Chem* 1980, **255:**7108-7117.

32. Howard AD, McAllister G, Feighner SD, Liu Q, Nargund RP, Van der Ploeg LH, Patchett AA: **Orphan G-protein-coupled receptors and natural ligand discovery.** *Trends Pharmacol Sci* 2001, **22:**132-140.

33. Civelli O, Nothacker HP, Saito Y, Wang Z, Lin SH, Reinscheid RK: **Novel neurotransmitters as natural ligands of orphan G-protein-coupled receptors.** *Trends Neurosci* 2001, **24:**230-237.

34. Dohlman HG, Thorner J, Caron MG, Lefkowitz R: **Model systems for the study of seven-transmembrane-segment receptors.** *Annu Rev Biochem* 1991, **60:**653-688.

35. Christopoulos A: **Allosteric binding sites on cell-surface receptors: novel targets for drug discovery.** *Nat Rev Drug Disc* 2002, **1:**198-210.

36. Taipale J, Cooper MK, Maiti T, Beachy PA: **Patched acts catalytically to suppress the activity of Smoothened.** *Nature* 2002, **418:**892-897.

37. Bourne HR: **How receptors talk to trimeric G proteins.** *Curr Opin Cell Biol* 1997, **9:**134-142.

38. DeCamp D, Thompson TM, de Sauvage FJ, Lerner MR: **Smoothened activates Galphai-mediated signaling in frog melanophores.** *J Biol Chem* 2000, **275:**26322-26327.

39. Trousse F, Marti E, Gruss P, Torres M, Bovolenta P: **Control of retinal ganglion cell axon growth: a new role for Sonic hedgehog.** *Development* 2001, **128:**3927-3936.

40. Carstea ED, Morris JA, Coleman KG, Loftus SK, Zhang D, Cummings C, Gu J, Rosenfeld MA, Pavan WJ, Krizman DB, *et al.*: **Niemann-Pick C1 disease gene: homology to mediators of cholesterol homeostasis.** *Science* 1997, **277:**228-231.

41. Hampton RY: **Cholesterol homeostasis: ESCAPe from the ER.** *Curr Biol* 2000, **10:**R298-R301.

42. Davies JP, Chen FW, Ioannou YA: **Transmembrane molecular pump activity of Niemann-Pick C1 protein.** *Science* 2000, **290:**2295-2298.

43. Traiffort E, Charytoniuk DA, Faure H, Ruat M: **Regional distribution of Sonic Hedgehog, patched, and smoothened mRNA in the adult rat brain.** *J Neurochem* 1998, **70:**1327-1330.

44. Parmantier E, Lynn B, Lawson D, Turmaine M, Namini SS, Chakrabarti L, McMahon AP, Jessen KR, Mirsky R: **Schwann cell-derived Desert hedgehog controls the development of peripheral nerve sheaths.** *Neuron* 1999, **23:**713-724.

45. St-Jacques B, Dassule HR, Karavanova I, Botchkarev VA, Li J, Danielian PS, McMahon JA, Lewis PM, Paus R, McMahon AP: **Sonic hedgehog signaling is essential for hair development.** *Curr Biol* 1998, **8:**1058-1068.

46. Sato N, Leopold PL, Crystal RG: **Induction of the hair growth phase in postnatal mice by localized transient expression of Sonic hedgehog.** *J Clin Invest* 1999, **104:**855-864.

47. Pola R, Ling LE, Silver M, Corbley MJ, Kearney M, Pepinsky RB, Shapiro R, Taylor FR, Baker DP, Asahara T, Isner JM: **The morphogen Sonic hedgehog is an indirect angiogenic agent upregulating two families of angiogenic growth factors.** *Nat Med* 2001, **7:**706-711.

48. Vortkamp A, Pathi S, Peretti GM, Caruso EM, Zaleske DJ, Tabin CJ: **Recapitulation of signals regulating embryonic bone formation during postnatal growth and in fracture repair.** *Mech Dev* 1998, **71:**65-76.

49. Pepinsky RB, Shapiro RI, Wang S, Chakraborty A, Gill A, Lepage DJ, Wen D, Rayhorn P, Horan GS, Taylor FR, *et al.*: **Long-acting forms of Sonic hedgehog with improved pharmacokinetic and pharmacodynamic properties are efficacious in a nerve injury model.** *J Pharm Sci* 2002, **91:**371-387.

50. Tsuboi K, Shults CW: **Intrastriatal injection of sonic hedgehog reduces behavioral impairment in a rat model of Parkinson's disease.** *Exp Neurol* 2002, **173:**95-104.

51. Chen JK, Taipale J, Cooper M, Beachy PA: **Inhibition of Hedgehog signaling by direct binding of cyclopamine to Smoothened.** *Genes Dev* 2002, **16:**2743-2748.

52. Chen JK, Taipale J, Young JE, Maiti T, Beachy PA: **Small molecule modulation of Smoothened activity.** *Proc Natl Acad Sci USA* 2002, **99:**14071-14076.